

Supporting Informations

Nanozyme Composite with High Near-Infrared Photothermal Ability for Synergistic Bacterial Elimination

Jing Liu,^{*a} Ruke Wang,^a Fenfen Zhai,^a Wengan Zhang^a, Bo Wang^{*a} and Hong Zhou^{*b}

^aCollege of Chemical and Biological Engineering, Shandong University of Science and Technology, Qingdao, 266590, PR China.

^bShandong Key Laboratory of Biochemical Analysis; College of Chemistry and Molecular Engineering, Qingdao University of Science and Technology, Qingdao 266042, China.

**E-mail: jingliu@sdust.edu.cn (J. Liu); wb@sdust.edu.cn (B. Wang); zhouhong@qust.edu.cn (H. Zhou)*

Table of contents

Figure S1. Transmission electron microscopy (TEM) images of rGO-Au NFs S3

Figure S2. Comparison of photothermal conversion efficiency between Hemin-rGO@Au NFs, rGO@Au NFs and ultrapure water under irradiation with 808 nm laser. S4

Figure S3. Comparison of catalytic activity between Hemin-rGO@Au NFs and rGO@Au NFs. S5

Figure S4. The stability of Hemin-rGO@Au NFs in catalytic activity. S6

Figure S5. Catalytic activity changes of Hemin-rGO@Au NFs after irradiation treatment. S7

Figure S6. The toxicity of Hemin-rGO@Au NFs with different concentrations on normal cell lines (measured by CCK8 assay). S8

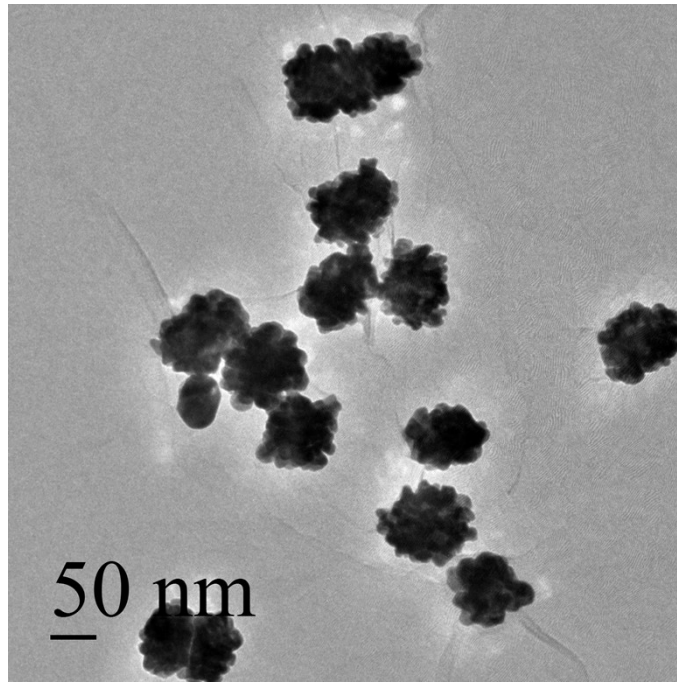


Figure S1. Transmission electron microscopy (TEM) images of rGO-Au NFs.

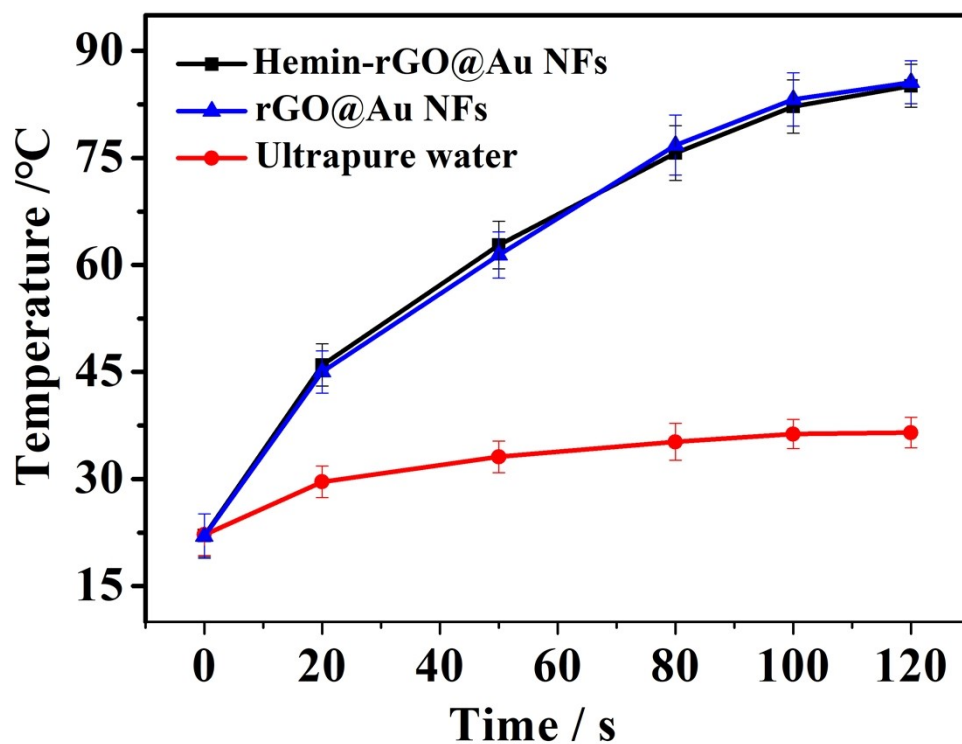


Figure S2. Comparison of photothermal conversion efficiency between Hemin-rGO@Au NFs, rGO@Au NFs and ultrapure water under irradiation with 808 nm laser.

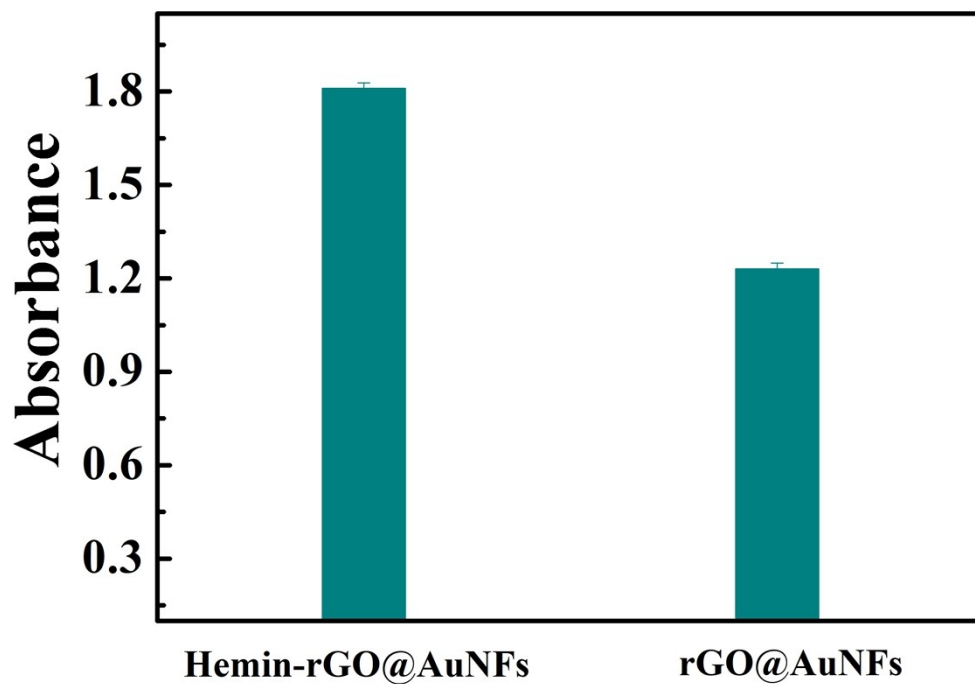


Figure S3. Comparison of catalytic activity between Hemin-rGO@Au NFs and rGO@Au NFs.

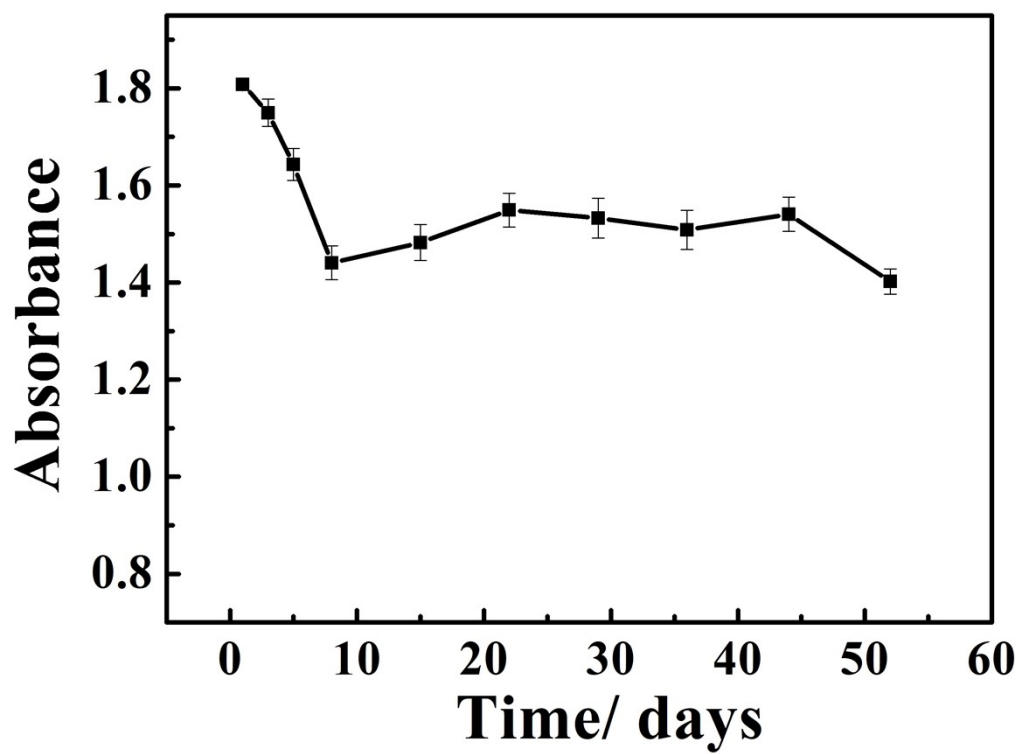


Figure S4. The stability of Hemin-rGO@Au NFs in catalytic activity.

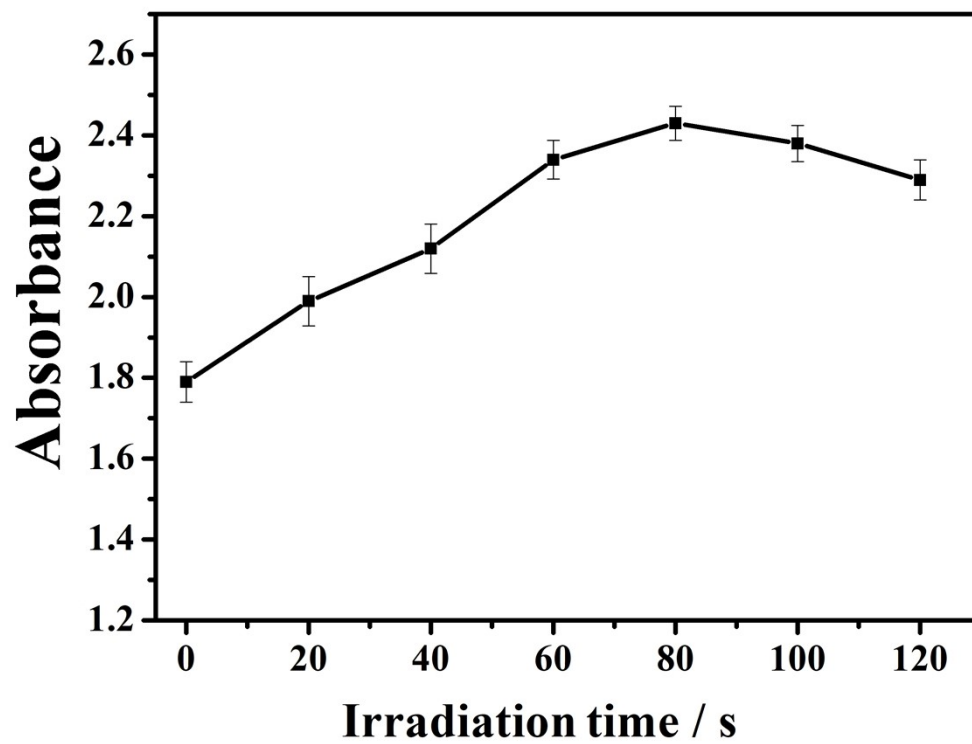


Figure S5. Catalytic activity changes of Hemin-rGO@Au NFs after irradiation treatment.

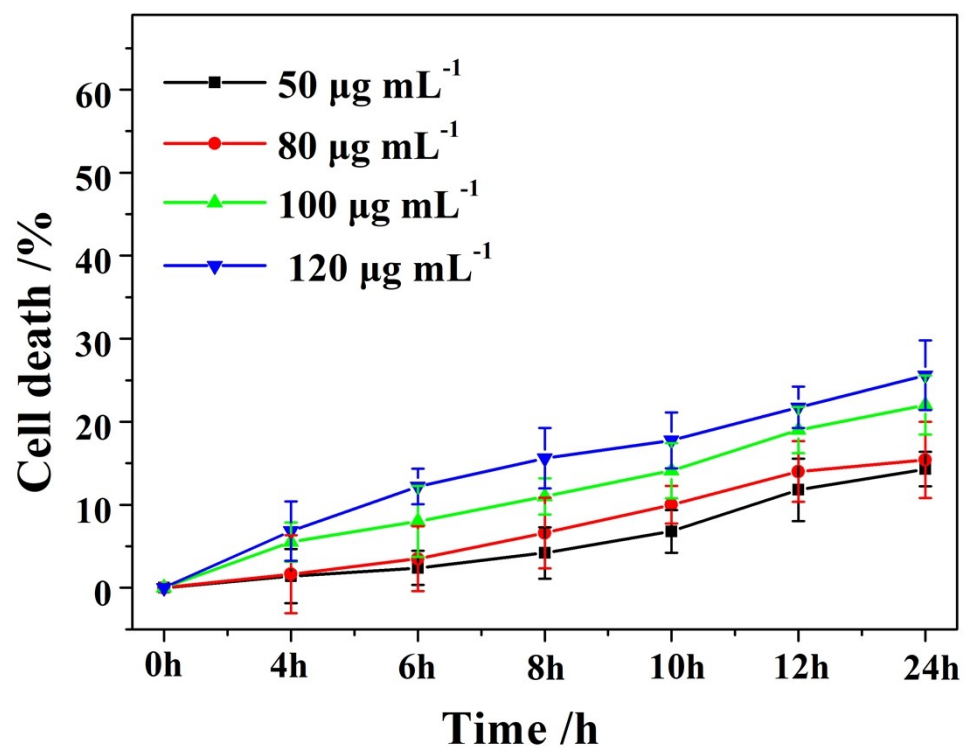


Figure S6. The toxicity of Hemin-rGO@Au NFs with different concentrations on normal cell lines (measured by CCK8 assay).